doi: 10.1002/osp4.297

ORIGINAL ARTICLE

Estimation of visceral fat in 9- to 13-year-old girls using dual-energy X-ray absorptiometry (DXA) and anthropometry

V. Lee[1], R. Blew[1], M. Hetherington-Rauth[1], D. Blew[2], J.-P. Galons[3], T. Hagio[4,5], J. Bea[1,6], T. Lohman[2] and S. Going[1]

[1]Department of Nutritional Sciences, University of Arizona, Tucson, Arizona, USA; [2]Department of Physiology, University of Arizona, Tucson, Arizona, USA; [3]Department of Medical Imaging, University of Arizona, Tucson, Arizona, USA; [4]Department of Biomedical Engineering, University of Arizona, Tucson, Arizona, USA; [5]Division of Imaging, Diagnostics, and Software Reliability, Center for Devices and Radiological Health, U.S. Food and Drug Administration, Silver Spring, Maryland, USA; [6]Department of Medicine, University of Arizona, Tucson, Arizona, USA.

Received 1 May 2018; revised 23 July 2018; accepted 1 August 2018

Address for correspondence: Vinson Lee, Department of Nutritional Sciences, University of Arizona, 3950 S, Country Club Road, Tucson, Arizona 85714, USA. E-mail: vinsonl@email.arizona.edu

Summary

Objectives

Accumulation of visceral fat (VF) in children increases the risk of cardiovascular disease and type 2 diabetes, and measurement of VF in children using computed tomography and magnetic resonance imaging (MRI) is expensive. Dual-energy X-ray absorptiometry (DXA) may provide a low-cost alternative. This study aims to determine if DXA VF estimates can accurately estimate VF in young girls, determine if adding anthropometry would improve the estimate and determine if other DXA fat measures, with and without anthropometry, could be used to estimate VF in young girls.

Methods

Visceral fat was measured at lumbar intervertebral sites (L1–L2, L2–L3, L3–L4 and L4–L5) using 3.0T MRI on 32 young girls (mean age 11.3 ± 1.3 years). VF was estimated using the GE CoreScan application. Measurement of DXA android and total body fat was performed. Weight, height and waist circumference (WC) measurements were also obtained.

Results

Waist circumference and body mass index were both strongly correlated with MRI, although WC was the best anthropometric covariate. Per cent fat (%fat) variables had the strongest correlation and did best in regression models. DXA %VF (GE CoreScan) and DXA android %fat and total body %fat accounted for 65% to 74% of the variation in MRI VF.

Conclusion

Waist circumference predicted MRI VF almost as well as DXA estimates in this population, and a combination of WC and DXA fat improves the predictability of VF. DXA VF estimate was improved by the addition of WC; however, DXA android %fat with WC was better at predicting MRI VF.

Keywords: Imaging, Obesity, Paediatric, Visceral fat.

Introduction

Childhood and adolescent obesity, with its attendant health risks, remains at an all-time high (1). In youth, as in adults, a growing body of evidence suggests fat distribution, as much as, if not more so than whole-body fat, confers risk of cardio-metabolic diseases (2–5). For example, accumulation of visceral fat (VF) in adolescents is associated with metabolic syndrome and an increased risk of cardiovascular disease and type 2 diabetes (2–4,6).

Accurate measurement of VF is difficult to achieve, and measurement of VF in large studies requires a fast and inexpensive method that is accessible, valid and accurate. Anthropometric surrogates of VF (e.g. body mass index [BMI], waist circumference [WC] and waist–hip ratio) have proven to be less than ideal measures and tend to be

better correlated with total fat than VF (7–9). Direct methods for measuring VF, such as computed tomography (CT) and magnetic resonance imaging (MRI) (10,11), are expensive and have limited access, especially for conducting large population-based studies. Additionally, the radiation exposure associated with CT is a concern, especially in pre-pubertal and pubertal children.

Dual-energy X-ray absorptiometry (DXA), which has been used to measure total and regional whole-body composition for many years, offers a low radiation alternative (11). Early work in late teens and adults combined a DXA fat measurement (total fat, android fat, etc.) plus an anthropometric measurement (BMI, WC, etc.) in an equation to estimate VF (12,13). Recent advances have now led to a 'fully automated' DXA measurement of VF and have provided a low radiation exposure alternative to CT and a low-cost alternative to both CT and MRI. GE Lunar and Hologic instruments both offer VF measurements from total body DXA scans using proprietary software applications such as GE Lunar's CoreScan and Hologic's InnerCore applications. Both have been validated against CT in adults but not in children. Whether these equations can be applied in youth is not clear. Thus, total body scans were obtained using a GE Lunar densitometer and estimated VF using CoreScan in 32 adolescent girls. The primary aim was to determine the accuracy of the GE Lunar CoreScan application for estimation VF in adolescent girls using MRI as the criterion method. A secondary aim was to determine whether the addition of anthropometric measures to DXA VF improved the estimation of MRI VF. A tertiary aim was to determine if other DXA measures of adiposity could be used to estimate VF in young girls and if these estimates are improved with the addition of anthropometric measures.

Methods

Study population

Thirty-two healthy adolescent girls with diverse body composition, aged 9–13 years, who were participants in the 'Soft Tissue and Bone Development in Young Girls (STAR)' study were studied. The STAR study was designed to assess the effects of adiposity and related metabolic risk factors on bone development. Exclusion criteria included diagnosis of diabetes, taking any medications that alter body composition, physical disability that limits physical activity and learning disability that limited completion of questionnaires or otherwise made the participant unable to comply with assessment protocols. The study protocol was approved by the University of Arizona Human Subjects Protection Committee. Written informed consent was obtained from all participants and their parents or legal guardians. All body composition measurements, blood draw and questionnaires were completed at the Body Composition Research Laboratory in the Collaboratory for Metabolic Disease Prevention and Treatment at the University of Arizona.

Anthropometric measures

Body weight was measured to the 0.1 kg with a calibrated digital scale (Seca, Model 881, Hamburg, Germany). Standing height was measured to the nearest 0.1 cm using a stadiometer (Shorr Height Measurement Board, Olney, MD). WC was measured to the nearest 0.5 cm at the umbilicus using an anthropometric tape. All measurements were performed in duplicate, and the average of the measurements was used in the analysis. BMI was calculated using the measured height and weight of each participant. Maturity offset was estimated from age and anthropometric measures (height, weight, sitting height and leg length) using the validated Mirwald equation (14).

Dual-energy X-ray absorptiometry acquisition

Measures of whole-body (total fat mass and total per cent fat) and regional adiposity (android fat mass and android per cent fat) were obtained from DXA using the GE/Lunar Prodigy densitometer (GE Healthcare, Madison, WI) following standard subject positioning and data acquisition protocols. The android region of interest (ROI) is defined as the regions with its inferior border at the iliac crest and superior border defined by 20% of the distance between this point and immediately below the chin and laterally to include all of the torso (15). The within-subject variation for bone and soft tissue for the Lunar Prodigy DXA machine has been previously reported (16). The Prodigy densitometer was calibrated daily according to the manufacturer guidelines. All DXA scans were conducted by trained operators, and all analyses were performed by one certified technician.

Dual-energy X-ray absorptiometry visceral fat measurement

Dual-energy X-ray absorptiometry visceral fat was calculated using GE Lunar's CoreScan application, which utilizes a validated algorithm that estimates the mass and volume of VF in the android region (15). This application has a lower age limit of 18 years; thus, to test the application in this sample of young girls, actual birthdates were adjusted so that all participants would appear to be 18 years of age so that an estimate of VF could be obtained.

Magnetic resonance imaging acquisition

All MRI examinations were performed on a 3T MR system (MAGNETOM Skyra, Siemens Healthcare, Erlangen, Germany). Imaging was performed using an anterior 18-channel flexible array coil in combination with 12–16 elements of the table-mounted spine array. For the abdomen, the two-point Dixon (17) 3D VIBE sequence (breath-hold) was used with the following parameters: TR = 3.92 ms, flip angle = 10, matrix 288 × 168, field of view 380–420 mm, slice thickness = 3.5 mm, 96 partitions, phase resolution 70%, slice resolution 50%, bandwidth = 1300 Hz per pixel, bipolar readout, the first TE = 1.23 ms (out of phase) and the second echo at 2.46 ms (in phase). A parallel acceleration technique (CAIPIRINHA) was used with acceleration factors of 2 in both phase encoding and partition directions, leading to an acquisition time of 13 s (17). Contiguous 3.5-mm slices from L1 to S1 were obtained for all participants.

Magnetic resonance imaging sites for estimation of visceral fat

From the literature, it is evident that 'best site' often depends on numerous factors (18–26). For MRI VF, segmentation was performed on four intervertebral slices, between L1 and L2 (L1–L2), L2 and L3 (L2–L3), L3 and L4 (L3–L4) and L4 and L5 (L4–L5), in order to observe the association with DXA measures of adiposity and subsequently select the slices best correlated with MRI VF.

Magnetic resonance imaging image segmentation

Image segmentation of MRI slices was accomplished using a graphical user interface (GUI) developed using MATLAB programming (Mathworks, Natick, MA). The GUI provides semi-automatic ROI image segmentation of fat. The GUI provides the technician with a user-adjustable thresholding feature based on signal intensity. Threshold level was selected to allow inclusion of fat while excluding lean tissue (e.g. muscle and organs). The use of the 'Add more ROI' and 'Erase region' functions allows the technician to adjust the segmentation in areas that needed modification to include or exclude pixels from ROIs. The semi-automatic feature is the separation of the subcutaneous fat from the VF after ROI manipulation is complete. Upon completion, the segmented image is saved as a colour-rendered image with the subcutaneous fat in yellow and the VF in red – colours converted to greyscale for publication (Figure 1). The

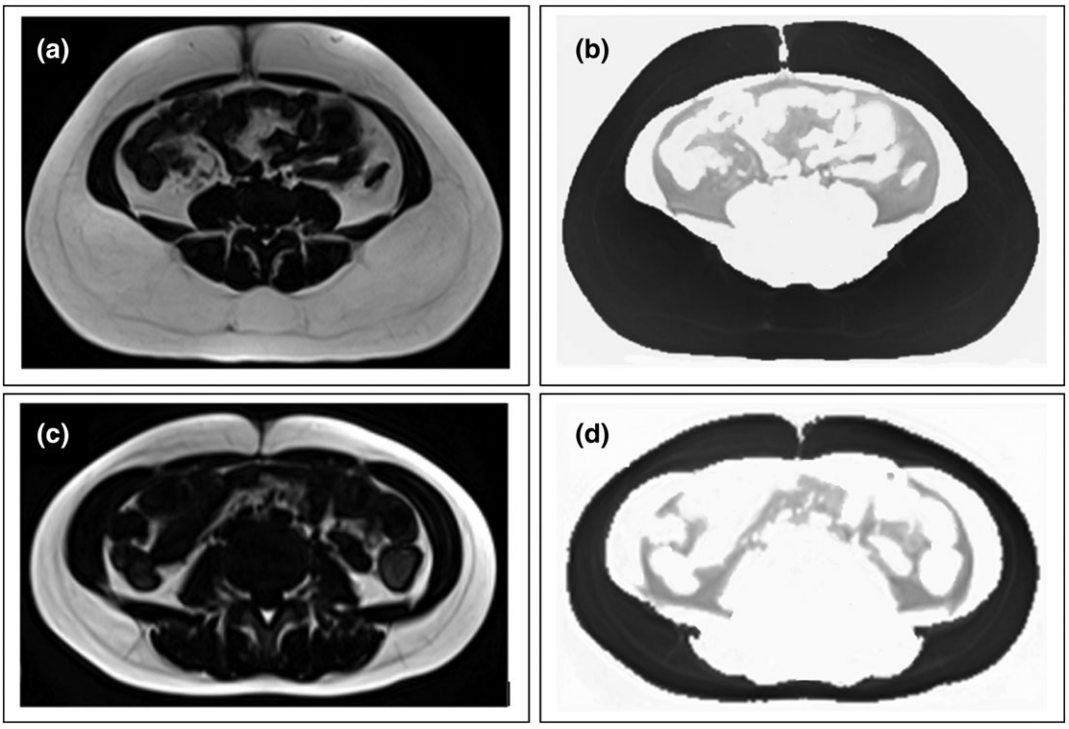

Figure 1 Pairs a/b and c/d show unsegmented (left; a and c) and segmented (right; b and d) magnetic resonance imaging slices (dark grey = subcutaneous fat; grey = visceral fat in segmented images).

number of pixels in both the subcutaneous and VF ROIs is tallied and saved. When the segmentation of all slices was completed, the GUI generates a report that provides the total number of pixels counted in subcutaneous and VF ROIs for each slice.

Segmentation was performed by two trained technicians. Each technician repeated segmentation on 10 randomly selected participants (one-third of total subjects) in order to determine intra-rater reliability. Inter-rater and intra-rater intraclass correlations were high ($R \geq 0.98$).

Conversion of magnetic resonance imaging data to volume and mass

Pixel count was converted to voxel volume by multiplying the pixel dimensions and slice thickness. VF volume was then calculated by multiplying pixel count and voxel volume. The CoreScan software estimates and records the VF in mass (grams). Kaul *et al*. (15) used a conversion factor of 0.94 g cm^{-3} for all volume to mass conversions in their study. Because the goal was to compare the DXA measurement with MRI, the same conversion factor was used to estimate VF mass for all MRI slices.

Statistical analysis

Means and standard deviations were calculated for all sample characteristics. Measures of skewness and kurtosis were calculated to determine distribution characteristic of anthropometric variables. Linear regression was used to assess the relationship of MRI VF to DXA VF and also to assess the relationships of other body fat measures (android fat and total body fat) for DXA versus MRI VF.

Multiple regression analyses were used to test whether anthropometric variables (WC, BMI and weight) improved the prediction of MRI VF from DXA VF, android fat and total body fat. Age was added to each model as a surrogate for maturity.

Bland–Altman analysis was used to determine the level of agreement between MRI measures of VF and the VF estimations from the regression equations. Scatterplots with fit lines were constructed to aid in visualizing the relationship between the regression equation VF value and the MRI VF.

The Statistical Package for the Social Sciences (SPSS) 24.0 (IBM Corp., Armonk, NY) was used for all statistical analyses.

Results

Study sample characteristics are shown in Table 1. Participant age ranged from 9 to 13 years. Mean height and mean weight percentiles were 63.4% and 73.9%, respectively, based on national norms (27). Mean WC and BMI percentiles were 73% and 71.6%, respectively, based on national norms (27). Using weight categories based on BMI percentile, 17 participants were normal weight, while six and nine participants were overweight and obese, respectively. The study sample was normally distributed for height and WC although slightly skewed right (skewness = 1.4, standard error [SE] = 0.414) for weight and skewed right (skewness = 1.056, SE = 0.414) for BMI. Mean values (±standard deviation) of DXA measures of adiposity, total fat mass, total per cent fat, android fat mass and android per cent fat were 17.2 ± 8.8 kg, 34.8 ± 9.1%, 1.29 ± 0.80 kg and 39.3 ± 12.2%, respectively. DXA VF mass and volume measured by the CoreScan software application was 230 ± 220 g and 247.3 ± 237.4 cm^3, respectively. Single-slice MRI VF mass for the lumbar intervertebral sites ranged from 14.3 ± 6.1 g at the L4–L5 level to 18.5 ± 9.0 g at the L2–L3 level. Differences in MRI VF mass are due to differences in ROIs at the various intervertebral sites.

Dual-energy X-ray absorptiometry measures of adiposity were significantly ($\rho \leq 0.001$) correlated with MRI VF

Table 1 Sample characteristics (n = 32)

Characteristic	Mean ± SD	Range
Age (years)	11.3 ± 1.3	9.3–13.7
Height (cm)	149.8 ± 9.7	132.0–166.9
Weight (kg)	48.2 ± 13.1	27.5–92.9
BMI (kg m^{-2})	21.3 ± 4.3	15.3–33.4
BMI percentile (%)	71.6 ± 26.5	21.9–99.2
Waist circumference (cm)	77.4 ± 12.0	26.9–99.9
Waist percentile (%)	73.0 ± 25.8	18–99
Maturity offset (years)	0.9 ± 1.3	−1.4 to 2.6
DXA total body fat mass (kg)	17.2 ± 8.8	5.8–48.0
DXA total body per cent fat (%)	34.8 ± 9.1	16.4–52.8
DXA android fat mass[a] (kg)	1.29 ± 0.80	0.36–3.9
DXA android per cent fat[a] (%)	39.3 ± 12.2	15.4–60.1
DXA visceral fat mass[b] (g)	230 ± 220	20–890
DXA visceral fat volume[b] (cm^3)	247.3 ± 237.4	19.2–945.3
DXA visceral per cent fat[b] (%)	9.4 ± 6.6	1.2–23.0
MRI L1–L2 visceral fat mass (g)	16.5 ± 9.3	2.4–36.7
MRI L2–L3 visceral fat mass (g)	18.5 ± 9.0	4.3–40.3
MRI L3–L4 visceral fat mass (g)	16.7 ± 7.5	5.3–36.5
MRI L4–L5 visceral fat mass (g)	14.3 ± 6.1	6.2–29.3
MRI visceral fat mass sum[c] (g)	66.0 ± 30.7	18.6–135.2

[a]DXA android fat variables were measured using automatic ROI for android region.
[b]DXA visceral fat were measured using CoreScan software.
[c]MRI visceral fat mass sum = sum of four slices (L1–L2 + L2–L3 + L3–L4 + L4–L5).
BMI, body mass index; DXA, dual-energy X-ray absorptiometry; MRI, magnetic resonance imaging; ROI, region of interest; SD, standard deviation.

Table 2 Correlations between MRI and DXA variables (n = 32)

MRI variable	DXA VFM[a]	DXA VPF[a]	DXA AFM	DXA APF	DXA TBFM	DXA TBPF	WC	BMI	Weight
MRI VFM L1–L2	0.71	0.77	0.72	0.82	0.69	0.83	0.74	0.75	0.51
MRI VFM L2–L3	0.70	0.77	0.70	0.81	0.66	0.79	0.72	0.70	0.51
MRI VFM L3–L4	0.75	0.82	0.76	0.85	0.73	0.84	0.81	0.75	0.57
MRI VFM L4–L5	0.79	0.82	0.77	0.81	0.76	0.83	0.84	0.80	0.63
MRI VFM sum[b]	0.76	0.82	0.76	0.85	0.73	0.85	0.80	0.78	0.57

$\rho \leq 0.001$ for all correlations. DXA android fat variables were measured using automatic ROI for android region.
[a]DXA visceral fat variables were estimated using GE Lunar's CoreScan application.
[b]MRI VFM sum = sum of four slices (L1–L2 + L2–L3 + L3–L4 + L4–L5).
BMI, body mass index; DXA, dual-energy X-ray absorptiometry; DXA AFM, dual-energy X-ray absorptiometry android fat mass; DXA APF, dual-energy X-ray absorptiometry android per cent fat; DXA TBFM, dual-energy X-ray absorptiometry total body fat mass; DXA TBPF, dual-energy X-ray absorptiometry total body per cent fat; DXA VFM, dual-energy X-ray absorptiometry visceral fat mass, DXA VPF, dual-energy X-ray absorptiometry visceral per cent fat; MRI, magnetic resonance imaging; ROI, region of interest; VFM, visceral fat mass; WC, waist circumference.

measurements (Table 2). DXA VF mass (VFM), android fat mass (AFM) and total body mass (TBFM) were all similarly correlated with MRI VF. DXA measures of android per cent fat (APF) and total body per cent fat (TBPF) were more highly correlated with MRI VF than DXA visceral per cent fat (VPF). WC, BMI and body weight (weight) were significantly correlated ($\rho \leq 0.001$) with MRI VF measurements. WC had a higher association with MRI VF than BMI and body weight (Table 2).

Table 3 Regression of DXA visceral fat, DXA android fat[a] and DXA total body fat variables on MRI visceral fat variables (n = 32)

Dependent	Predictor	Adjusted R^2	SEE	%SEE
MRI VFM L4–L5	DXA VFM	0.61	3.8	26.6
MRI VFM sum[b]	DXA VFM	0.57	20.1	30.5
MRI VFM L4–L5	DXA VPF	0.65	3.6	25.2
MRI VFM sum[b]	DXA VPF	0.66	17.8	27.0
MRI VFM L4–L5	DXA AFM	0.59	3.9	27.3
MRI VFM sum[b]	DXA AFM	0.56	20.2	30.6
MRI VFM L4–L5	DXA APF	0.64	3.6	25.2
MRI VFM sum[b]	DXA APF	0.72	16.2	24.5
MRI VFM L4–L5	DXA TBFM	0.57	4.0	28.0
MRI VFM sum[b]	DXA TBFM	0.52	21.2	32.1
MRI VFM L4–L5	DXA TBPF	0.68	3.5	24.3
MRI VFM sum[b]	DXA TBPF	0.72	16.2	24.5

All mass values in grams.
[a]DXA android fat variables were measured using automatic ROI for android region.
[b]MRI visceral fat mass sum = sum of four slices (L1–L2, L2–L3, L3–L4 and L4–L5).
DXA, dual-energy X-ray absorptiometry; DXA AFM, dual-energy X-ray absorptiometry android fat mass; DXA APF, dual-energy X-ray absorptiometry android per cent fat; DXA TBFM, dual-energy X-ray absorptiometry total body fat mass; DXA TBPF, dual-energy X-ray absorptiometry total body per cent fat; DXA VFM, dual-energy X-ray absorptiometry visceral fat mass, DXA VPF, dual-energy X-ray absorptiometry visceral per cent fat; MRI, magnetic resonance imaging; ROI, region of interest; SEE, standard error of the estimate; VFM, visceral fat mass.

The results of simple univariate regression of DXA measures of adiposity on MRI VF mass (MRI VFM) are shown in Table 3. In general, significant associations were found but were lower for L1–L2, L2–L3, L3–L4 compared with L4–L5 and MRI VF sum as shown in Table 2, and thus, only the results for MRI VF at L4–L5 and MRI VF sum are shown in this table and all subsequent tables. DXA VPF variables had consistently higher adjusted R^2 values and lower standard error of the estimate (SEE) values than DXA VFM. Overall, DXA VF variables performed comparably with DXA android fat variables and DXA total fat variables resulting in similar adjusted R^2 values and SEE values (Table 3). Per cent fat variables were more highly correlated than fat mass variables for all MRI VF sites and provide better adjusted R^2 and SEE values across all regressions. Regression models that used per cent fat variables had consistently better adjusted R^2 values and lower SEE values compared with models that used fat mass variables.

Table 4 compares regression models where DXA, anthropometry and age were regressed on MRI VF variables. Only the results for MRI VF at L4–L5 and MRI VF sum are shown. The addition of WC and BMI to DXA measures of adiposity improved the adjusted R^2 values in almost all regression models (Table 4). Additionally, adding age did not improve the adjusted R^2 in all models and was only significant in some of the models. When age was significant, it often resulted in the loss of significance in the DXA variable, anthropometric variable or both. The addition of body weight did not improve prediction of MRI VF variables (data not shown).

The addition of anthropometric measures and age to DXA VF models, however, did not improve prediction of MRI VF variables compared with models using DXA android and DXA total body measures. Furthermore, DXA

Table 4 DXA measures of adiposity[a] and anthropometry regressed on MRI VFM variables with and without age in the models (n = 32)

		Predictor(s)					
		DXA VPF + WC	DXA APF + WC	DXA TBPF + WC	DXA VPF + BMI	DXA APF + BMI	DXA TBPF + BMI
Dependent	Age covariate	Adjusted R^2	Adjusted R^2	Adjusted R^2	Adjusted R^2	Adjusted R^2	Adjusted R^2
MRI VFM L4–L5	Without	0.71[e]	0.72[d]	0.71[d]	0.71[d]	0.71[d]	0.69[d]
	With	0.71[e]	0.72[e]	0.72[e]	0.70[d]	0.70[d]	0.69[d]
MRI VFM sum[b]	Without	0.68[c]	0.74[d]	0.72[c]	0.69[c]	0.74[c]	0.72[c]
	With	0.70[e]	0.74[d]	0.74[c]	0.70[d]	0.74[c]	0.73[c]

This table only shows the results of regressions performed with DXA per cent fat variables because they had the highest adjusted R^2 and lowest SEE values when compared with DXA fat mass variables.

[a]DXA measures of adiposity: DXA APF, dual-energy X-ray absorptiometry android per cent fat; DXA TBPF, dual-energy X-ray absorptiometry total body per cent fat; DXA VPF, dual-energy X-ray absorptiometry visceral per cent fat. DXA android fat variables were measured using automatic ROI for android region.

[b]MRI VFM sum = sum of four slices (L1–L2 + L2–L3 + L3–L4 + L4–L5).

[c]DXA variable was significant ($p \leq 0.05$) in regression model; however, anthropometric variable and/or age was not significant.

[d]DXA and anthropometric variables were significant ($p \leq 0.05$) in regression model.

[e]Anthropometric variable was significant; however, DXA and/or age were not significant.

BMI, body mass index; DXA, dual-energy X-ray absorptiometry; MRI, magnetic resonance imaging; ROI, region of interest; VFM, visceral fat mass; WC, waist circumference.

VF variables were 'intermittently' significant ($p > 0.05$) after the addition of anthropometric variables and age. Regression models that included body weight as a predictor had consistently lower adjusted R^2 values than models using WC and BMI and were left out of Table 4.

Selected regression models

The regression equations with the greatest adjusted R^2 values and the lowest SEEs are summarized in Table 5. All selected models included WC as the anthropometric measure as it performed better than BMI. Age was included in all models to control for maturity. Keeping 'age' in the regression model generally improved the adjusted R^2 only slightly and did not improve SEE over models without age as a covariate. Regressions were also performed with maturity offset (an alternate measure of maturity) in place of age. Regression outcomes using maturity offset were similar to models using age (data not shown). Models that included WC performed best, whereas models that included body weight as a covariate had consistently lower adjusted R^2 and higher SEE values (data not shown).

Scatterplots and Bland–Altman plots of selected regression models

Scatterplots (Figure 2) provide a comparison between DXA VPF and DXA APF of how well each predicts MRI VFM. The first four plots in Figure 3a–d are scatterplots

Table 5 Regression equations giving the best prediction of MRI VFM

Model	Equation	Adjusted R^2	SEE	%SEE
1	MRI VFM L4–L5 = (0.229 * DXA VPF[a]) + (0.315 * WC) − (0.534 * age) − 6.26	0.71	3.3	22.9
2	MRI VFM sum[b] = (1.410 * DXA VPF[a]) + (1.372 * WC) − (4.796 * age) − 0.35	0.70	16.7	25.3
3	MRI VFM L4–L5 = (0.136 * DXA APF[a]) + (0.308 * WC) − (0.428 * age) − 10.00	0.72	3.2	22.4
4	MRI VFM sum[b] = (1.206 * DXA APF[a]) + (1.017 * WC) − (3.139 * age) − 24.62	0.74	15.6	23.6
5	MRI VFM L4–L5 = (0.215 * DXA TBPF[a]) + (0.280 * WC) − (0.485 * age) − 9.33	0.72	4.0	27.8
6	MRI VFM sum[b] = (1.670 * DXA TBPF[a]) + (0.927 * WC) − (3.990 * age) − 18.60	0.74	15.6	23.6

Model numbers are arbitrary.

[a]DXA measures of adiposity: DXA APF, dual-energy X-ray absorptiometry android per cent fat; DXA TBPF, dual-energy X-ray absorptiometry total body per cent fat; DXA VPF, dual-energy X-ray absorptiometry visceral per cent fat. DXA android fat variables were measured using automatic ROI for android region.

[b]MRI VFM sum = sum of four slices (L1 − L2 + L2 − L3 + L3 − L4 + L4 − L5).

DXA, dual-energy X-ray absorptiometry; MRI, magnetic resonance imaging; ROI, region of interest; SEE, standard error of the estimate; VFM, visceral fat mass; WC, waist circumference.

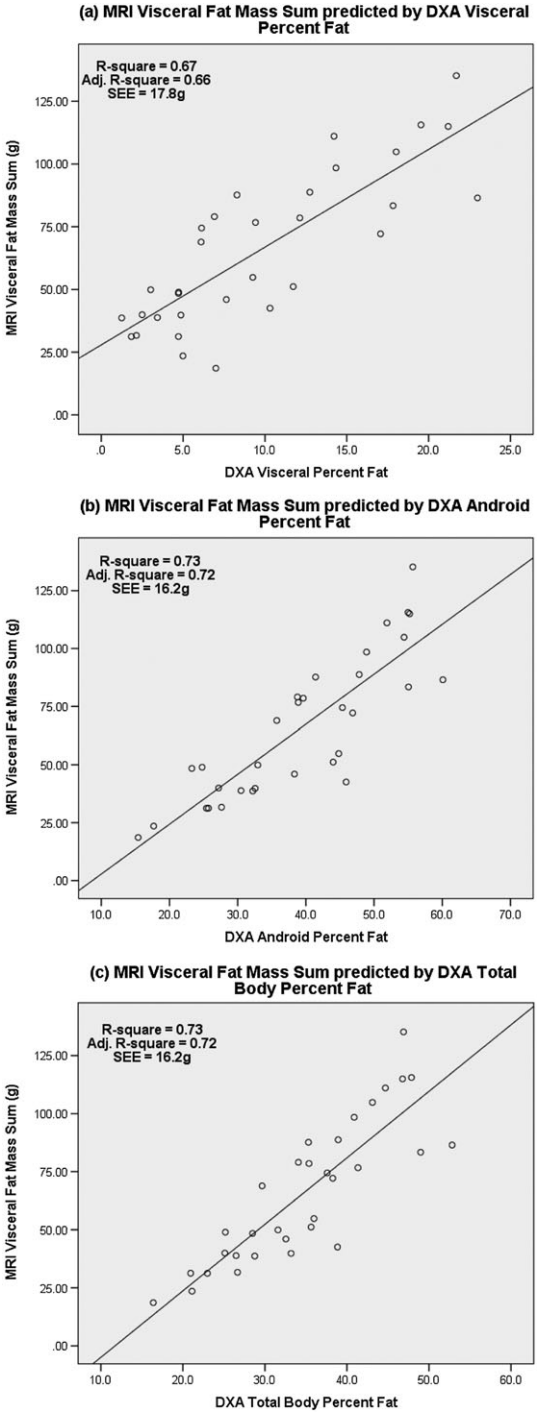

Figure 2 (a) Relationship between magnetic resonance imaging visceral fat mass (MRI VFM) sum (g) and dual-energy X-ray absorptiometry (DXA) visceral per cent fat (%) estimated by the GE Lunar CoreScan application, (b) relationship between MRI VFM sum (g) and the measured DXA android per cent fat (%) and (c) relationship between MRI VFM sum (g) and the measured DXA total body per cent fat (%). SEE, standard error of the estimate.

and Bland–Altman plots for model 4 and model 6, which had the highest adjusted R^2 of all the 'best' models when predicting MRI VFM sum. Scatterplots and Bland–Altman plots show good agreement between the regression equation estimates and MRI VFM. Eror plots, which plot the regression equation results against the error (MRI values minus predicted values) for model 4 and model 6, are shown in Figure 3e,f, respectively. In general, the error plots show that error increases with higher amounts of VF.

Because of slight but noticeable curvilinear character exhibited in scatterplots of DXA versus MRI, analysis of the variability was performed on the DXA measures of adiposity. The DXA mass variables (VFM, AFM and TBFM) were skewed right (1.42–1.63; SE = 0.414) with some kurtosis (1.63–3.92; SE = 0.809). Of the per cent fat variables, only DXA VPF was slightly skewed right (0.618; SE = 0.806). Log transformation of these variables did not improve regression outcomes. Analysis of variability was also performed on MRI VF variables, which found the MRI variables to have a fairly normal distribution with very little skewness or kurtosis.

Discussion

This study sought to determine whether DXA estimates of VF using GE Lunar's CoreScan software application are accurate in young girls (aged 9–13 years). This software estimate of VF was previously validated in an adult sample by Kaul *et al*. (15), using the criterion measure of abdominal X-ray CT in 109 adult participants. Other successful estimations of VF in adults using DXA have been made in recent years using MRI as the criterion method with studies reporting that VF measurement by DXA is strongly correlated with MRI VF (28–31). None of these studies included children in their sample.

This study is the only one to examine the applicability of the GE CoreScan software application in children. Correlation analysis showed that DXA measures of fat mass (VFM, AFM and TBFM) were moderately correlated (r = 0.43–0.59, $p < 0.001$) with MRI VF in girls aged 9–13 years. These results are similar to those of Laddu *et al*. who did not have VF estimating software but compared the fat masses of both an automatically drawn DXA android ROI and a manually drawn DXA ROI of the L1 to L4 region, to MRI VF at the L4–L5 level in a sample of men and women aged 12–25 year (32). They showed that with the addition of gender and/or weight, 54% to 62% of the variance in VF could be explained (32). VF estimates provided by the GE Lunar CoreScan application accounted for 48% to 61% of the variation in MRI VF at all intervertebral sites as well as the sum of the slices regardless of whether the DXA VF was

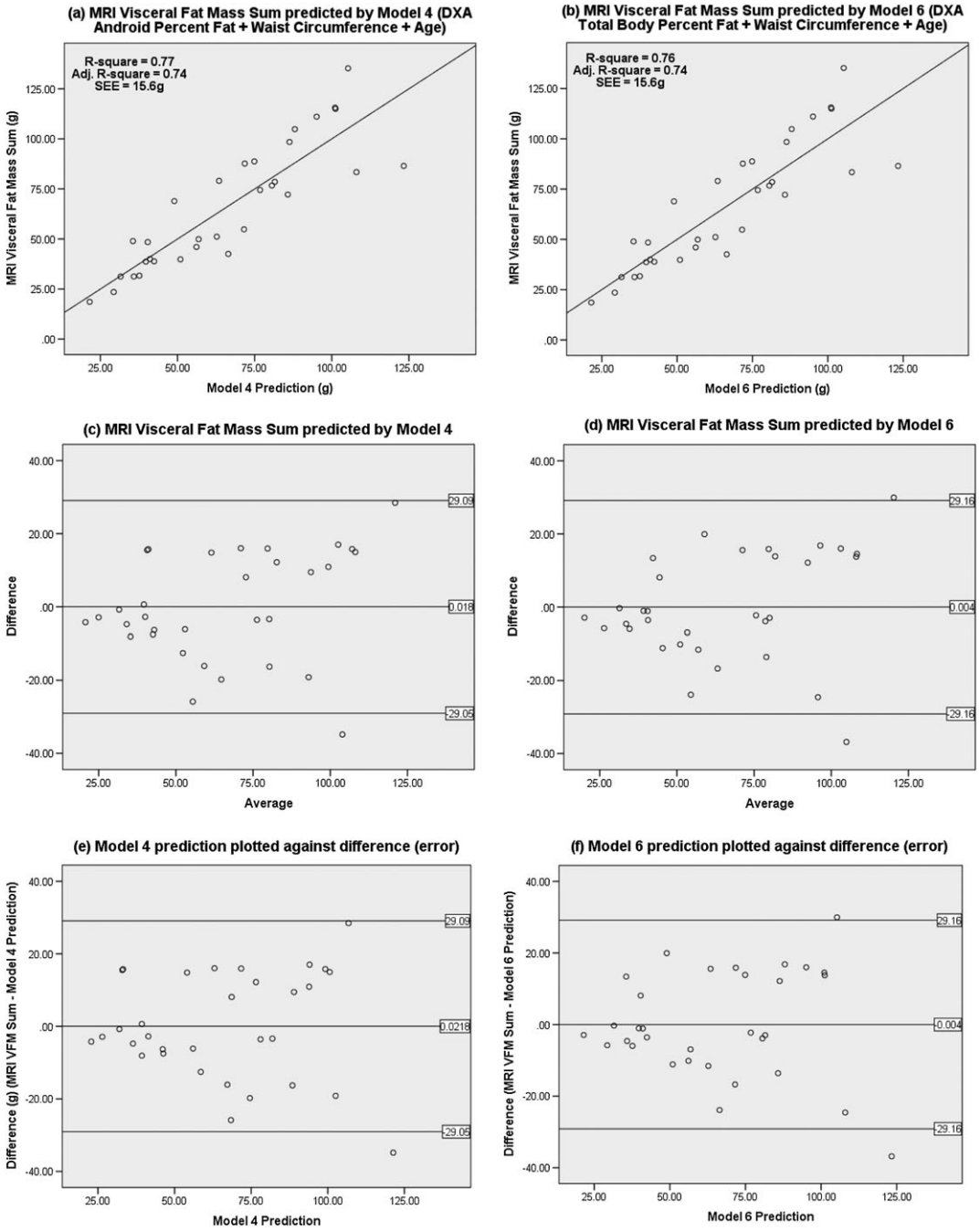

Figure 3 (a) Relationship between magnetic resonance imaging visceral fat mass (MRI VFM) sum (g) and VF predicted by model 4 (Table 5), (b) relationship between MRI VFM sum (g) and VF predicted by model 6, (c) Bland–Altman plot of the difference and average of MRI VFM sum and model 4 prediction, (d) Bland–Altman plot of the difference and average of MRI VFM sum and model 6 prediction, (e) plot of model 4 VFM prediction against error (MRI VFM sum − model 4 prediction) and (f) plot of model 6 VFM prediction against error (MRI VFM sum − model 6 prediction). SEE, standard error of the estimate.

expressed in mass or as a per cent. Simple univariate regressions using DXA android fat mass and DXA TBFM as the predictors provided similar results when compared with the DXA VF regressions.

Dual-energy X-ray absorptiometry per cent fat variables were better correlated with MRI VF than DXA fat mass variables, with the exception of DXA VF. Additionally, simple regression showed that the predictive power

of DXA android per cent fat and DXA total body per cent fat was better than that of DXA VFM, DXA android fat mass and DXA total body fat mass. DXA android and total body per cent fat variables accounted for 62% to 72% of the variation in MRI VFM at all sites compared with 42% to 61% for the mass variables. DXA visceral per cent fat accounted for less variability compared with the other per cent fat variables, although it accounted for more variability than DXA VFM. It can be surmised that, in general, increased percentage of total body fat translates to increased VF content more than total fat mass because VF increases in relation to per cent fat (i.e. in participants with obesity) as opposed to those large participants who have more fat in total but not as a per cent.

Interestingly, there was an inverse relationship between age and VF predicted from DXA, indicating that in older girls for a given amount of DXA fat, there is less VF. In general, the relationship is non-significant, but in several models, it did approach significance. This relationship may be the result of the limited sample size, and a future study using a larger study population may prove this to be a significant finding.

This study also sought to determine whether adding simple anthropometric measurements to DXA VF and other DXA measures of adiposity can improve the estimation of VF. The GE CoreScan application used to estimate DXA VF in this study was not developed for this age group. Because it is a proprietary algorithm, it is not possible to know what specific variables are used in the application. An attempt was made to improve the ability for this application to estimate VF in this age group by including the anthropometric measurements of WC and BMI. Overall, the addition of anthropometric measures and age did improve prediction, but the prediction was not as good as using other DXA measures of adiposity (android per cent fat or total body per cent fat). Adding WC or BMI improved the adjusted R^2 and decreased the SEE in the majority of the models regardless of the DXA measure of adiposity. WC and BMI were both moderately correlated with MRI VF (waist = 0.72 to 0.84, $p < 0.001$; BMI = 0.70 to 0.80, $p < 0.001$). WC has been shown to be correlated with VF and is considered a predictor of VF, accounting for 65% of the variance in MRI VF (33), although some studies found WC to be a better predictor of subcutaneous fat and total fat (8,9,32). The relationship between BMI and VF, however, is inconsistent. Studies by Goodwin *et al*. and Ross *et al*. (8,32) had shown only low to moderate correlation; however, a study by O'Connor *et al*. (23) showed a strong correlation with VF. Body weight, on the other hand, was not as well correlated with MRI VF as WC and BMI.

In many regression models, the addition of WC or BMI resulted in the adiposity variable no longer being significant. WC is often used as a surrogate measure for estimating VF (33) and had stronger correlation than the DXA measure of adiposity in this study, and therefore, the adiposity variable losing significance would be a realistic consequence when adding WC to the models. Overall, WC was the most common anthropometric covariate appearing in models with the greatest adjusted R^2.

The findings of this study are limited by the small sample size and narrow age range of the participants (9–13 years; mean age = 11.3 ± 1.3 years). A larger sample size was not financially feasible because of the cost of MRI imaging. Additionally, a power analysis calculation could not be completed because of the lack of an effect size estimate on the bias of the DXA CoreScan software application as applied to the sample. However, the sample was diverse across a range of BMI and per cent body fat. Additionally, the narrow age range may limit the usefulness of the selected equations to be generalizable to older girls. A final limitation is that total VF measurements from MRI were not available for use in the analysis.

Conclusion

The results of this study show that there is a strong relationship between DXA measures of adiposity and MRI measures of VF. In univariate regression, the GE Lunar CoreScan application estimates VF in young girls 9–13 years of age comparatively as well as other DXA measures. Although the GE Lunar CoreScan application estimate can be improved by adding WC, other DXA measures of adiposity are better correlated and result in better estimation of VF, especially after adding WC. The results also indicate that WC alone is a good predictor of VF in young girls and that combining WC with DXA android per cent fat accounts for 74% of the variability in VF measured by MRI.

Although the resultant equations account for considerable variability with satisfactory SEE and %SEE, the use of these equations cannot be recommended. In order to improve these equations to provide a more accurate estimate, total MRI VF should be acquired in order to provide total VF measurement by the criterion method. Furthermore, future studies should include a greater number of participants with a more diverse range of body habitus, age, race and ethnicity.

Overall, this study shows that the association among DXA measures of adiposity and anthropometry can be combined to accurately estimate VF in young girls. Thus, it appears likely that a generalizable formula can be developed for girls improving on the present GE Lunar CoreScan application.

Funding

Support for this study was provided by the Eunice Kennedy Shriver National Institute for Child Health and Human Development grant R01 HD-074565.

Conflict of Interest Statement

The authors declare no conflict of interest.

Acknowledgements

We would like to thank the University of Arizona Collaboratory for Metabolic Disease Prevention and Treatment Center, where this investigation was completed, and the Arizona Cancer Center Imaging Core for support with the development of image processing tools.

We would like to thank Dr Hagio for developing the MRI segmentation program used to quantify VF for this study. Dr Hagio is currently at the U.S. Food and Drug Administration. The work herein was carried out when she was at the University of Arizona.

References

1. Hales CM, Carroll MD, Fryar CD, Ogden CL. Prevalence of obesity among adults and youth: United States, 2015–2016. *NCHS Data Brief* 2017: 1–8.
2. Kelly AS, Dengel DR, Hodges J, et al. The relative contributions of the abdominal visceral and subcutaneous fat depots to cardiometabolic risk in youth. *Clin Obes* 2014; **4**: 101–107.
3. Gower BA, Nagy TR, Goran MI. Visceral fat, insulin sensitivity, and lipids in prepubertal children. *Diabetes* 1999; **48**: 1515–1521.
4. Goran MI, Gower BA. Relation between visceral fat and disease risk in children and adolescents. *Am J Clin Nutr* 1999; **70**: 149S–156S.
5. Goran MI, Gower BA. Abdominal obesity and cardiovascular risk in children. *Coron Artery Dis* 1998; **9**: 483–487.
6. Goran MI, Ball GD, Cruz ML. Obesity and risk of type 2 diabetes and cardiovascular disease in children and adolescents. *J Clin Endocrinol Metab* 2003; **88**: 1417–1427.
7. Katzmarzyk PT, Bouchard C. Where is the beef? Waist circumference is more highly correlated with BMI and total body fat than with abdominal visceral fat in children. *Int J Obes (Lond)* 2014; **38**: 753–754.
8. Goodwin K, Syme C, Abrahamowicz M, et al. Routine clinical measures of adiposity as predictors of visceral fat in adolescence: a population-based magnetic resonance imaging study. *PLoS One* 2013; **8**: e79896.
9. Ribeiro-Filho FF, Faria AN, Azjen S, Zanella MT, Ferreira SR. Methods of estimation of visceral fat: advantages of ultrasonography. *Obes Res* 2003; **11**: 1488–1494.
10. Shuster A, Patlas M, Pinthus JH, Mourtzakis M. The clinical importance of visceral adiposity: a critical review of methods for visceral adipose tissue analysis. *Br J Radiol* 2012; **85**: 1–10.
11. Sasai H, Brychta RJ, Wood RP, et al. Does visceral fat estimated by dual-energy X-ray absorptiometry independently predict cardiometabolic risks in adults? *J Diabetes Sci Technol* 2015; **9**: 917–924.
12. Bertin E, Marcus C, Ruiz JC, Eschard JP, Leutenegger M. Measurement of visceral adipose tissue by DXA combined with anthropometry in obese humans. *Int J Obes Relat Metab Disord* 2000; **24**: 263–270.
13. Clasey JL, Bouchard C, Teates CD, et al. The use of anthropometric and dual-energy X-ray absorptiometry (DXA) measures to estimate total abdominal and abdominal visceral fat in men and women. *Obes Res* 1999; **7**: 256–264.
14. Mirwald RL, Baxter-Jones AD, Bailey DA, Beunen GP. An assessment of maturity from anthropometric measurements. *Med Sci Sports Exerc* 2002; **34**: 689–694.
15. Kaul S, Rothney MP, Peters DM, et al. Dual-energy X-ray absorptiometry for quantification of visceral fat. *Obesity (Silver Spring)* 2012; **20**: 1313–1318.
16. Going S, Lohman T, Houtkooper L, et al. Effects of exercise on bone mineral density in calcium-replete postmenopausal women with and without hormone replacement therapy. *Osteoporos Int* 2003; **14**: 637–643.
17. Ma J. Dixon techniques for water and fat imaging. *J Magn Reson Imaging* 2008; **28**: 543–558.
18. Bosch TA, Dengel DR, Kelly AS, Sinaiko AR, Moran A, Steinberger J. Visceral adipose tissue measured by DXA correlates with measurement by CT and is associated with cardiometabolic risk factors in children. *Pediatr Obes* 2015; **10**: 172–179.
19. Brown RE, Kuk JL, Lee S. Measurement site influences abdominal subcutaneous and visceral adipose tissue in obese adolescents before and after exercise. *Pediatr Obes* 2015; **10**: 98–104.
20. Ellis KJ, Grund B, Visnegarwala F, et al. Visceral and subcutaneous adiposity measurements in adults: influence of measurement site. *Obesity (Silver Spring)* 2007; **15**: 1441–1447.
21. Maislin G, Ahmed MM, Gooneratne N, et al. Single slice vs. volumetric MR assessment of visceral adipose tissue: reliability and validity among the overweight and obese. *Obesity (Silver Spring)* 2012; **20**: 2124–2132.
22. Kuk JL, Church TS, Blair SN, Ross R. Measurement site and the association between visceral and abdominal subcutaneous adipose tissue with metabolic risk in women. *Obesity (Silver Spring)* 2010; **18**: 1336–1340.
23. O'Connor M, Ryan J, Foley S. Best single-slice location to measure visceral adipose tissue on paediatric CT scans and the relationship between anthropometric measurements, gender and VAT volume in children. *Br J Radiol* 2015; **88** 20140711.
24. Schaudinn A, Linder N, Garnov N, et al. Predictive accuracy of single- and multi-slice MRI for the estimation of total visceral adipose tissue in overweight to severely obese patients. *NMR Biomed* 2015; **28**: 583–590.
25. Shen W, Punyanitya M, Wang Z, et al. Visceral adipose tissue: relations between single-slice areas and total volume. *Am J Clin Nutr* 2004; **80**: 271–278.
26. Sun J, Xu B, Freeland-Graves J. Automated quantification of abdominal adiposity by magnetic resonance imaging. *Am J Hum Biol* 2016; **28**: 757–766.
27. Fryar CD, Gu Q, Ogden CL, Flegal KM. Anthropometric reference data for children and adults: United States, 2011–2014. *Vital and Health Statistics* 2016; **3**: 1–46.
28. Neeland IJ, Grundy SM, Li X, Adams-Huet B, Vega GL. Comparison of visceral fat mass measurement by dual-X-ray absorptiometry

and magnetic resonance imaging in a multiethnic cohort: the Dallas Heart Study. *Nutr Diabetes* 2016; **6**: e221.
29. Taylor AE, Kuper H, Varma RD, et al. Validation of dual energy X-ray absorptiometry measures of abdominal fat by comparison with magnetic resonance imaging in an Indian population. *PLoS One* 2012; **7**: e51042.
30. Cheung AS, de Rooy C, Hoermann R, et al. Correlation of visceral adipose tissue measured by Lunar Prodigy dual X-ray absorptiometry with MRI and CT in older men. *Int J Obes (Lond)* 2016; **40**: 1325–1328.
31. Mohammad A, De Lucia RE, Sleigh A, et al. Validity of visceral adiposity estimates from DXA against MRI in Kuwaiti men and women. *Nutr Diabetes* 2017; **7**: e238.
32. Ross R, Leger L, Morris D, de Guise J, Guardo R. Quantification of adipose tissue by MRI: relationship with anthropometric variables. *J Appl Physiol (1985)* 1992; **72**: 787–795.
33. Brambilla P, Bedogni G, Moreno LA, et al. Crossvalidation of anthropometry against magnetic resonance imaging for the assessment of visceral and subcutaneous adipose tissue in children. *Int J Obes (Lond)* 2006; **30**: 23–30.